Uncorrected Proof

Journal of
Water & Climate Change

IWA PUBLISHING

Journal of Water and Climate Change Vol 00 No 0, 1 doi: 10.2166/wcc.2024.723

Limnological dynamics of methane (CH_4) and carbon dioxide (CO_2) emissions from a tropical hypertrophic reservoir lake

Oscar Gerardo-Nieto [a], Martin Merino-Ibarra [a,*], Salvador Sánchez-Carrillo [b], Andrea P. Guzmán-Arias [c], Fermín S. Castillo-Sandoval [a], Mariel Barjau-Aguilar [d], Patricia M. Valdespino-Castillo [a,e], Julio A. Lestayo-González [a], Julio Díaz-Valenzuela [a], Jorge Alberto Ramírez-Zierold [a] and Frédéric Thalasso [f]

[a] Unidad Académica de Ecología y Biodiversidad Acuática, Instituto de Ciencias del Mar y Limnología, Universidad Nacional Autónoma de México, México
[b] Departamento de Biogeoquímica y Ecología Microbiana, Museo Nacional de Ciencias Naturales, Consejo Superior de Investigaciones Científicas (MNCN-CSIC), España
[c] Posgrado de Ciencias del Mar y Limnología de la Universidad Nacional Autónoma de México, México
[d] Instituto de Geología, Universidad Nacional Autónoma de México, México
[e] Escuela Nacional de Ciencias de la Tierra, Universidad Nacional Autónoma de México, México
[f] Department of Biotechnology and Bioengineering, CINVESTAV, Mexico
*Corresponding author. E-mail: mmerino@cmarl.unam.mx

OG, 0000-0003-3299-9456; MM, 0000-0002-6690-3101; SS, 0000-0002-5471-977X; FSC, 0000-0002-5934-8859; MB, 0000-0001-5497-1249; PMV, 0000-0002-2998-4627; JAL, 0000-0002-7462-3118; JAR, 0000-0001-8094-1852; FT, 0000-0003-2246-2372

ABSTRACT

Methane (CH_4) and carbon dioxide (CO_2) emissions from tropical freshwater ecosystems have been understudied, particularly in terms of their interaction with limnological dynamics, their cycling, and the emission mechanisms of CH_4. To help reduce that knowledge gap, this study addressed these processes in Valle de Bravo (VB), a tropical (19° 11. 65′ N) reservoir lake, that provides water supply to Mexico City metropolitan area. CH_4 and CO_2 concentrations and emissions from VB were measured during four field campaigns distributed along the annual limnological cycle of the reservoir. Dissolved CH_4 concentration varied over four orders of magnitude (0.015–176.808 μmol L^{-1}), and dissolved CO_2 varied from below atmospheric saturation (15.062 μmol L^{-1}) to 10 times that concentration (219.505 μmol L^{-1}). CH_4 fluxes ranged from 23.25 to 1220.80 μmol m^{-2} day^{-1}, while CO_2 fluxes ranged from −60.11 to 254.99 mmol m^{-2} day^{-1}. Seasonal monitoring also allowed the assessment of the annual emissions as well as the greenhouse gas (GHG) storage during thermal stratification, which accounted for >58% of the total GHG annual emissions from VB. Overall, VB is a source of GHG, and its major contribution is the CH_4 released during the autumn overturn.

Key words: climate change, emissions, greenhouse gas, limnological dynamics, overturn, storage

HIGHLIGHTS

- The limnological dynamics of freshwater bodies have important effects on their GHG emissions
- Because of this, CH_4 emissions from VB varied seasonally by two orders of magnitude (23.25–1,220.80 μmol m^{-2} day^{-1}).
- Overall, VB was a net source of CH_4 and CO_2, but during stratification, it was a net sink of both GHGs.
- Most of the emissions were associated with the storage during the stratification period.

INTRODUCTION

Freshwater ecosystems are an important component in the global carbon cycle, because they store and release important amounts of carbon to the atmosphere. Although they cover barely 3.7% of the Earth's land surface (Verpoorter *et al.* 2014), continental freshwater ecosystems are responsible for about 16% of the total CH_4 emissions (Saunois *et al.* 2016), and 15% of the total CO_2 emissions to the atmosphere (Tranvik *et al.* 2009). In particular, in freshwater reservoirs, where there is a large stock of terrestrial organic matter due to both flooding and external loading, microbial decomposition may drive important production and emissions of CH_4 and CO_2 (Deemer *et al.* 2016).

The rate and the direction of CH_4 emission fluxes from freshwater ecosystems depend on the interlinkage of biological processes that affect the CH_4 budget with their limnological dynamics. Indeed, although the CH_4 concentration (C_{CH_4}) and CH_4 emission to the atmosphere are mainly a result of the balance between anaerobic CH_4 production (methanogenesis) and aerobic CH_4 oxidation (methanotrophy) (Miller *et al.* 2004), both of these processes may be differentially affected by the limnological structure and dynamics specific of the system, which can also affect the CH_4 transport and storage.

In freshwater ecosystems, methanogenesis takes place mainly in anaerobic sediments. It is the final step of the anaerobic degradation of organic material, which releases CH_4, and depends mainly of the availability of organic matter (Glissmann *et al.* 2004). In counterpart, methanotrophy also plays an important role in global methane cycling, mitigating the emissions of CH_4 through its oxidation to CO_2 and water. This process takes place mainly in oxic/anoxic interfaces, and it is carried out by methanotrophs, an important and specialized group of ubiquitous bacteria (Hrsak & Begonja 1998).

In terms of its emission pathways, CH_4 can reach the atmosphere by ebullition or by diffusion. Methane ebullition flux depends mainly on the net CH_4 production rate and on the hydrostatic pressure that the bubbles have to overcome to leave the sediments (Fendinger *et al.* 1992). In the case of CH_4 exported through diffusion from the sediments, CH_4 can be oxidized by methanotrophs as soon as it reaches oxic water (Bastviken *et al.* 2002). Additionally, the emission to the atmosphere depends on the concentration difference between the air and the water surface, but the exchange rate depends also on the turbulence driven by the wind speed (Podgrajsek *et al.* 2014). In stratified freshwater ecosystems, CH_4 can buildup in anoxic layers, until eventually this CH_4 storage can be emitted rapidly because of the full overturn of the system at the onset of the circulation period in monomictic freshwater ecosystems (Encinas Fernández *et al.* 2014). Additionally, CH_4 emissions might also occur and be significant in systems with high water level fluctuations (WLF) (Bartlett & Harriss 1993; Bartosiewicz *et al.* 2015, 2016) due to the short-term boundary mixing events that can occur during the stratification period in systems such as VB (Merino-Ibarra *et al.* 2021).

In the case of CO_2, the emission rates and the flux direction depend mainly on the trophic condition of the lake – the ratio of primary production to heterotrophic respiration (Guimarais-Bermejo *et al.* 2018), which are affected both by light penetration and the availability of inorganic nutrients and of organic matter (Bartosiewicz *et al.* 2016), dependent on the external loads it receives (Ramírez-Zierold *et al.* 2010) and the degree of eutrophication of the ecosystem, which in the case of VB is very high (Barjau-Aguilar *et al.* 2023). Additionally, the CO_2 budget is also affected by the allochthonous inputs of dissolved inorganic carbon coming from the weathering of mineral and soil respiration in the watershed (Marcé *et al.* 2015).

The majority of reports on CH_4 and CO_2 cycling dynamics in freshwater ecosystems are from temperate or boreal water bodies, while reports addressing this information in tropical water bodies are very scarce and heterogeneous. For example, in the global synthesis by Saunois *et al.* (2016), 83% of the >900 ecosystems they report on are located >50°N. Because of that, the assessment of greenhouse gas (GHG) dynamics in tropical aquatic ecosystems is crucial to reach a full understanding about global GHG balances, particularly because, as recognized by different studies (Bartlett & Harriss 1993; Merino-Ibarra *et al.* 2008), CH_4 emissions from tropical aquatic ecosystems may represent more than a half of the global emissions. Holgerson & Raymond (2016) have specifically addressed and outlined the critical lack of data on the CH_4 and CO_2 cycling dynamics under the 30° latitudes.

For these reasons, measuring CH_4 and CO_2 dynamics and emissions in reservoirs where these processes and fluxes have not been assessed is important to achieve both tropical and global understandings of the budgets of these GHG. This assessment is particularly needed for the numerous reservoirs throughout the world that receive high loads of organic matter and nutrients, as is the case of VB (Ramírez-Zierold *et al.* 2010), where GHG emissions are likely enhanced by the fueling additional of decomposition (Deemer *et al.* 2016).

It is also important to address the processes that may drive significant variations in these emissions, as is the case of WLF, a condition that affects numerous reservoirs because of water management or hydroelectric withdrawals, but also as a result of sharp local variations in rainfall and droughts derived from climate change. Independently of their origin, these high WLF may in turn cause high variations in the mechanisms and magnitude of GHG emissions, through hydrostatic pressure effects, but also through the impact of boundary mixing events that intensify during low water levels (Merino-Ibarra *et al.* 2008, 2021).

Therefore, the objectives of the present work are to measure both the dissolved concentrations of CH_4 and CO_2 as well as the magnitude and direction of their atmospheric fluxes in order to assess the annual cycling dynamics of these two GHG and their variability, mainly on the seasonal scale, in the hypertrophic monomictic tropical reservoir of VB, a system that is

important in itself and is also likely representative of many other reservoirs that are increasingly turning toward a higher trophic condition.

With these results, we expect to contribute to a better understanding of the processes that take place in tropical water bodies under eutrophication and water level pressures, and the variability that their CH_4 and CO_2 concentrations and emissions may undergo as a consequence of these processes. These results can in turn also be useful to improve the global estimates of GHG, and specifically global estimation of carbon fluxes, and the relative importance of tropical freshwater ecosystems for these fluxes and budgets.

METHODS

Study area and sampling campaigns

VB (19°11′39″N, 100°09′11″W; Figure 1) is a tropical reservoir lake located at 1,830 m a.s.l., 127 km west of Mexico City Metropolitan Area, to which it provides water supply (Ramírez-Zierold *et al.* 2010). The reservoir has a maximum superficial area of 18.55 km^2, a mean depth of 21.1 m, a maximum depth of 38.6 m near the dam, and a maximum water capacity of 392×10^3 m^3 (Merino-Ibarra *et al.* 2008). The climate in the VB region is sub-humid, warm to temperate with pronounced dry (November–May) and rainy season (June–October). This reservoir lake is characterized by a strong diurnal wind that blows along its two main valleys, which make it ideal for sailing and one of the most popular inland water resorts in Mexico (Merino-Ibarra *et al.* 2008). This tropical reservoir is very dynamic, so data on its emissions might likely contrast with previous reports (Holgerson & Raymond 2016), and therefore contribute to improving the representativeness of tropical ecosystems (Saunois *et al.* 2016) on global estimations of greenhouse gases (GHG) dynamics.

The selection of the VB reservoir for this study on GHG exchange also relied on the availability of limnological and biogeochemical data derived from the long-term monitoring of this system (Guimarais-Bermejo *et al.* 2018; Merino-Ibarra *et al.* 2021; Barjau-Aguilar *et al.* 2022) that has been ongoing since 2001. In previous studies, the lake's features, bathymetry, and its spatial variability were initially studied with an extensive, high-density network of sampling stations (17) distributed throughout the lake (Merino-Ibarra *et al.* 2008) to figure out the possible intricacy of the lake. Similarly, the influence of the four main

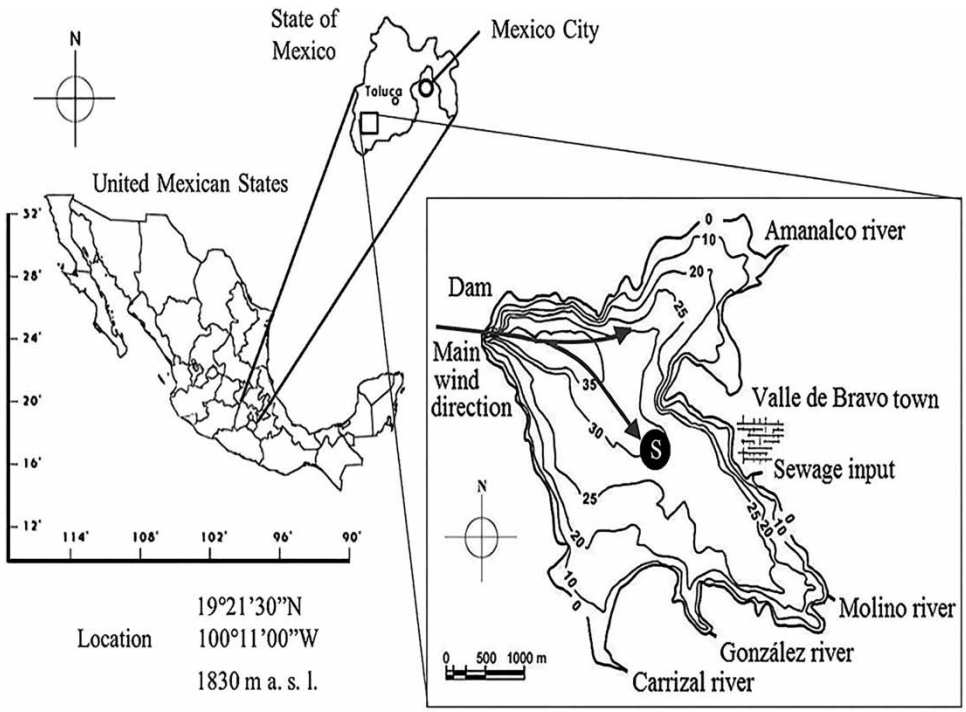

Figure 1 | Location and bathymetry of the Valle de Bravo (VB) reservoir (after Valeriano-Riveros *et al.* 2014). The black circle (S) indicates the sampling station.

rivers and sewages that discharge to VB was addressed in detail in a study of its N and P mass budgets and external loading (Ramírez-Zierold *et al.* 2010).

In these studies, it was found the lake is daily homogenized by the strong daily winds that blow in VB and that totally mix and homogenize its surface layer (Merino-Ibarra *et al.* 2008; Ramírez-Zierold *et al.* 2010). Functional studies on the primary production and community metabolism of the lake (Valdespino-Castillo *et al.* 2014) showed that this homogenization encompasses the metabolic processes and exchange fluxes (i.e., Guimarais-Bermejo *et al.* 2018; Barjau-Aguilar *et al.* 2023). Therefore, since 2008 VB monitoring has been realized using a single central station (Figure 1) which was shown to be representative of the lake in these previous works.

The CH_4 and CO_2 seasonal dynamics of the VB reservoir were therefore assessed at this long-term monitoring station (S in Figure 1) during four monitoring campaigns separated by 3-month intervals in seasonally characteristic months: April 2019 (early stratification period), July 2019 (stratification period), October 2019 (just before mixing period), and January 2020 (mixing period). Taking into account that the marked diel wind pattern of VB (Merino-Ibarra *et al.* 2008), which during the strong wind daytime period might bring GHG-rich water from the hypolimnion to the epilimnion (Merino-Ibarra *et al.* 2021), and trigger bubble release from the sediment (Podgrajsek *et al.* 2014), in each monitoring campaign GHG concentrations and emissions were studied both before and after the onset of these strong diurnal winds (i.e., ~11:00 and ~17:00) to include the influence of this wind diel pattern on GHG cycling in VB. Additionally, as part of the ongoing long-term monitoring of the reservoir underway (Merino-Ibarra *et al.* 2021), physicochemical parameters were monitored monthly throughout 2019 and 2020.

Physicochemical characteristics

Depth was measured using a portable sounder (Depthmate Portable Sounder, Speedtech, USA). Temperature, pH, and dissolved oxygen (DO) were measured at depth intervals of 1 m from the surface to the sediments using a multi-parametric probe (Yellow Spring Instruments model 6600, USA). Secchi depth was measured with a standard disk. Water densities derived from surface and bottom water temperatures were used to calculate the relative water column stability (RWCS; Padisák *et al.* 2003) with Equation (1), where D_B is the density of bottom water, D_S is the density of surface water, and D_4 and D_5 are the densities of water at 4 and 5 °C, respectively (Kalff 2002). According to Branco *et al.* (2009), freshwater ecosystems with an RWCS above 56.5 can be considered fully stratified, ecosystems those with an RWCS below 16.3 can be considered fully mixed, and ecosystems with RWCs between both can be considered partially mixed.

$$\mathrm{RWCS} = \frac{D_B - D_S}{D_4 - D_5}, \tag{1}$$

The thermocline depth was inferred from the water column stability, following Coloso *et al.* (2011). The oxycline depth was identified, when present, by the sharpest DO gradient and/or the presence of an oxic/anoxic gradient.

Dissolved GHG concentration

Dissolved CH_4 (C_{CH_4}) and CO_2 (C_{CO_2}) concentrations in the surface and the bottom of the reservoir were determined using the standard headspace equilibrium method (Magen *et al.* 2014). Briefly, this method consists on taking 40 mL of the water samples in a 60 mL syringe, adding 20 mL of He, and then vigorously shaking for at least 5 min to allow for gas/liquid equilibration. The mixed liquid is then evacuated, and 20 mL of the syringe headspace is transferred to a 12 mL Exetainer (Labco, UK) to be later measured in the laboratory. The CH_4 and CO_2 concentrations in the water sample were determined from the headspace concentrations by applying Henry's law, as given in Equation (2), where C_w is the dissolved gas in the water sample (CH_4 or CO_2; μmol L^{-1}), C_g^* is the gas concentration measured in the Exetainer of the sample in the headspace of the equilibrium syringe (μmol L^{-1}), V_l and V_g are the water and gas volumes in the syringe, respectively (L), H' is the CH_4 and CO_2 air/water partition coefficient (–), defined in Equation (3) where T is the water temperature (K), $H_{298.15}$ is the standard Henry constant (at 298.15 K), and τ is the temperature dependence constant. The values of $H_{298.15}$ and τ were obtained from Linstrom & Mallard (2016).

$$C_w = \frac{(C_g^* \cdot V_g) + \left(\frac{C_g^*}{H'} \cdot V_l\right)}{V_l} \tag{2}$$

$$H' = H_{298.15} \cdot e^{\tau\left(\frac{1}{T} - \frac{1}{298.15}\right)}, \quad (3)$$

CH_4 and CO_2 fluxes

CH_4 and CO_2 fluxes were determined in each campaign with the closed static floating chamber technique (SC; Livingston & Hutchinson 1995) using plastic HDPE buckets with a rubber septum and surrounded by foaming for their proper flotation. Three gas samples of the headspace SC were taken at 15 min intervals with 20 mL syringes and were immediately transferred to an Exetainer to be later measured in the laboratory. Fluxes were determined using Equation (4) where F is the flux (mmol m^{-2} day^{-1}), ΔC is the change in CH_4 or CO_2 concentration observed in the SC over the time interval (Δt), and V_{SC} and A_{SC} are the volume and contact surface area of the SC, respectively.

$$F = \frac{\Delta C}{\Delta t} \cdot \frac{V_{CDC}}{A'_{CDC}} \quad (4)$$

Although the SC method measures the total flux at the surface and includes both diffusive and ebullitive fluxes. Diffusive fluxes are characterized by a linear behavior of CH_4 or CO_2 concentrations in the SC headspace, while ebullition fluxes are characterized by a sudden step increase of CH_4 or CO_2 concentrations when a bubble reaches the SC headspace. In areas deeper than 20 m, such as the VB sampling site, ebullition fluxes are infrequent (Natchimuthu *et al.* 2016), because the depth of the water column favors GHG dissolution. To verify this in VB, visual long-term (>1 h) observations of the area were performed prior to the flux measurements, and after the flux measurements, an assessment of the linearity of the slope of the gas concentration was performed, because poor correlations can reveal the occurrence of ebullition or a lack of airtightness in the chamber. Each flux determination was done in triplicate.

Laboratory measurements

CH_4 and CO_2 analyses were made using an ultraportable greenhouse gas analyzer (UGGA, model 915-0011, Los Gatos Research, Inc., USA) and manual injection of the samples to an open circuit with a continuous flow of CH_4- and CO_2-Free nitrogen (Infra, Mexico) as a carrier gas, regulated at 1.5 L min^{-1} by a mass flow controller (GFC17, Alborg, Denmark). All the tubing used in the circuit was made of polyurethane with a 6 mm external diameter (Festo, Mexico). Additionally, gas samples were measured by gas chromatography using an Agilent 7890A GC system in order to test accuracy. The gas chromatography system was configured with a single channel using two detectors (FID and micro-ECD) for the analysis of CO_2 and CH_4. The total CH_4 and CO_2 emissions from the reservoir were calculated using the mean flux measurements before and after the onset of the strong diurnal wind and the surface area of the reservoir during each campaign.

Data analyses and statistics

The results obtained are presented as the average ± one standard deviation. Additionally, temporal contour maps of T, DO, and RWCS were plotted using Surfer 11.0 software (Golden Software, USA). The best method of interpolation based on the mean absolute error (MAE) and the mean bias error (MBE; (Willmott & Matsuura 2006)) was used. Since C_{CH_4}, C_{CO_2}, DO, and GHG fluxes were not normally distributed and did not meet the assumption of homoscedasticity, data were compared (e.g., among season and water depths) using the Mann–Whitney U test. Prior to correlation analysis, the data were normalized using logarithmic base 10 transformation, and linear regression analysis was used to quantify relationships. Before and after transformation, the data were tested for normality using the Shapiro–Wilk test. All statistics analyses were done with the NCSS200 Statistical Analysis System software (Number Crucher Statistical System, Utah, USA).

RESULTS AND DISCUSSION

Water level and water storage of VB

Table 1 summarizes the physicochemical data measured in VB during 2019–2020. Water levels changed seasonally in VB during this period due to seasonal rainfall variations and the water withdrawal from the reservoir for human use in Mexico City, Toluca, and other metropolitan areas. The water volume of the reservoir varied smoothly during this period, it was 85, 76, 81, and 95% (April, July, October, and January, respectively) of the maximum capacity of VB (391×10^6 m^3,

Table 1 | Valle de Bravo reservoir water storage and physicochemical parameters

Month	Apr (stratification)	Jul (stratification)	Oct (stratification)	Jan (circulation)
A_w (km^2)	16.53	15.74	16.11	17.61
Z_{max} (m)	34.3	32.4	33.4	36.1
V ($\times 10^6$ m^3)	332.97	297.02	314.78	370.94
RWCS[a]	88.85 (S)	95.36 (S)	47.59 (S)	15.61 (M)
T (°C)	19.72 ± 1.04	21.41 ± 1.24	21.96 ± 0.63	19.32 ± 0.13
DO[b] (μmol L^{-1})	237.7 ± 38.7	276.1 ± 56.7	210.0 ± 22.1	160.2 ± 0.94
pH (–)	8.29 ± 0.55	8.25 ± 0.53	8.77 ± 0.17	7.88 ± 0.49
SD (m)	1.30 ± 0.00	0.83 ± 0.32	1.10 ± 0.00	2.83 ± 0.32

A_w, surface area; Z_{max}, maximum depth; V, volume; RWCS, relative water column stability; T, temperature; DO, dissolved oxygen.
[a]RWCS: M, mixed; PS, partially stratified; S, stratified.
[b]DO above oxycline.

Merino-Ibarra *et al.* 2008), and the reservoir area was 89, 85, 87, and 95% relative to its maximum area (18.55 km^2 Merino-Ibarra *et al.* 2008). The depth at the sampling site also varied slightly, it was 26 m, 24, 25, and 28 m, respectively, for each of the monitoring campaigns (April, July, October, and January).

Physicochemical characterization

Figure 2 summarizes the vertical and temporal variation of temperature along the annual cycle in VB. The thermocline was located at approximately 13, 10, and 12 m of depth during April, July, and October, respectively. Temperature and RWCS

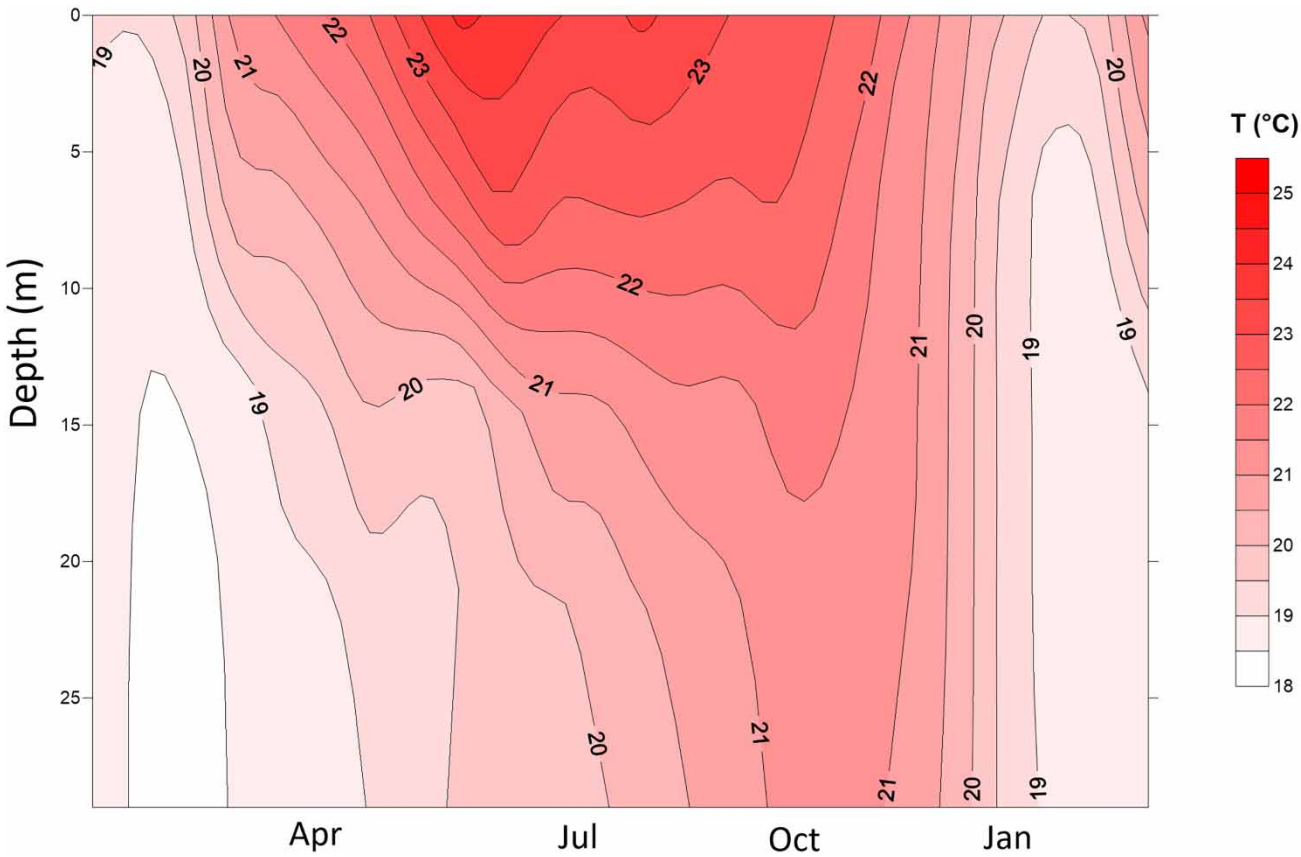

Figure 2 | Temperature vertical distribution from January 2019 to March 2020 in Valle de Bravo.

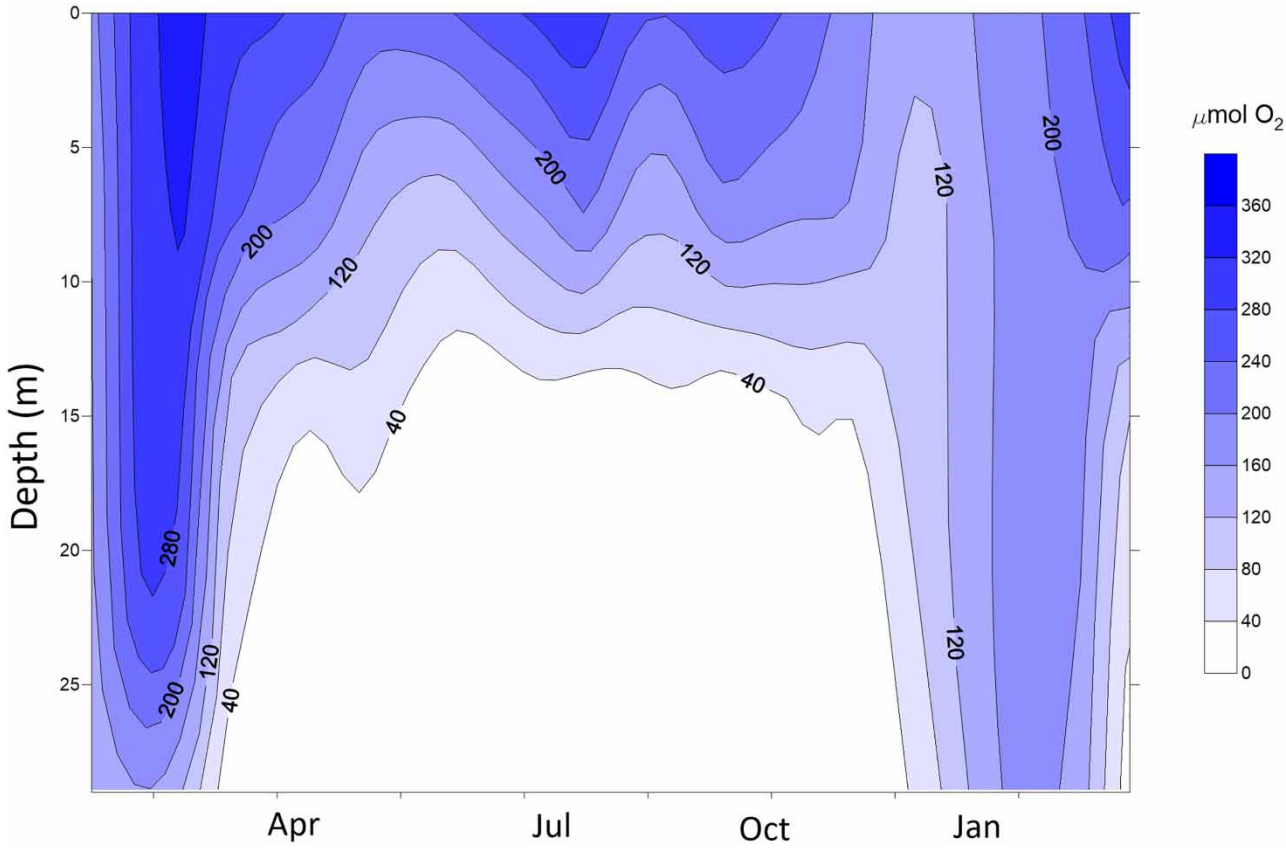

Figure 3 | Dissolved oxygen vertical distribution in Valle de Bravo from January 2019 to March 2020.

calculations obtained during parallel monthly monitoring (Merino-Ibarra *et al.* 2021) demonstrated that during 2019, the water column of VB began its stratification in March, reaching its maximum stability during May, and mixed vertically between October and November (Figure 2, also shown in Figures 4 and 5). RWCS values in Table 1 highlight that during January, VB was fully mixed.

Table 1 also summarizes other physicochemical parameters measured in VB during this period. pH ranged from 7.88 ± 0.49 (whole water column average) during January to 8.76 ± 0.17 during October, showing a chemocline at the same depth of the thermocline, and a vertical pH gradient when thermal stratification occurred (i.e., during July pH was 8.75 ± 0.16 in the epilimnion and 7.69 ± 0.19 in hypolimnion). The Secchi depth ranged from 0.60 to 3.05 m, reaching its minimum in July (at noon, after the onset of the diurnal wind) and its maximum in January (before the onset of the diurnal wind), values which are in agreement with the conditions found in eutrophic lakes (Vollenweider & Kerekes 1982).

Dissolved gases dynamics

Figure 3 demonstrates that the vertical and temporal variation of DO concentration in VB was tightly coupled to the stratification/circulation cycle of the reservoir, as shown by temperature. During April, July and October a strong oxycline was observed, below which totally anoxic conditions were registered, while during January, the full water column of the reservoir was partially oxygenated.

The C_{CH_4} measured in VB during 2019–2020 varied over more than four orders of magnitude: from 0.015 to 176.808 μmol L^{-1}, particularly between the surface and bottom layers when the reservoir was stratified (Figure 4(b)). The C_{CH_4} annual surface average was 0.132 ± 0.107 μmol L^{-1}, while the bottom C_{CH_4} averaged 62.585 ± 71.786 μmol L^{-1} when the reservoir was stratified. The C_{CH_4} at the bottom was significantly higher than that observed at the surface during the stratification ($p < 0.05$). Nevertheless, the C_{CH_4} data obtained for VB are overall still within the range previously reported for tropical hypertrophic freshwater ecosystems (Holgerson & Raymond 2016).

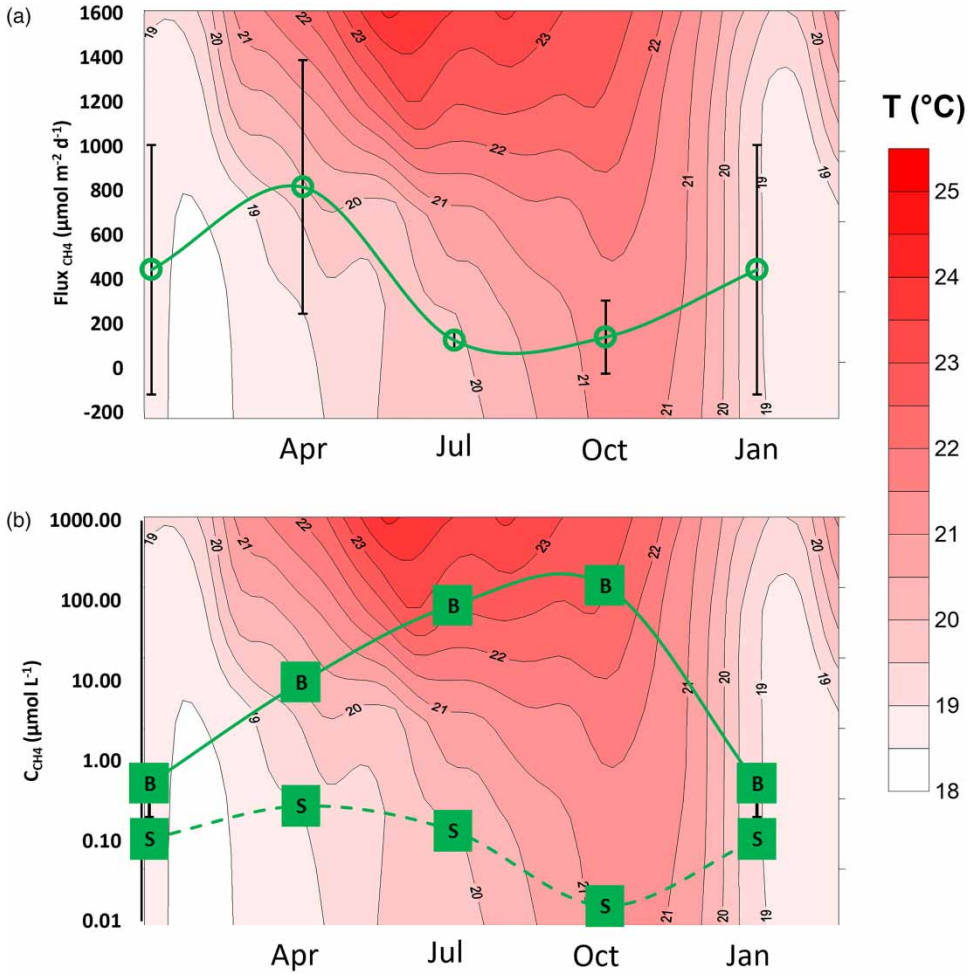

Figure 4 | CH_4 seasonal dynamics in Valle de Bravo: (a) seasonal variation of mean CH_4 fluxes, and (b) seasonal variation of C_{CH_4}. Dashed line and S symbols indicate mean surface C_{CH_4}, and solid line and B symbols indicate bottom C_{CH_4}. Vertical lines depict the standard deviation. The temperature vertical distribution is shown behind the plots to help outline the effect of the limnological dynamics of the lake reservoir on the gas concentration and fluxes.

C_{CH_4} exhibited a trend similar to that of DO, in which the highest differences between surface and bottom C_{CH_4} were observed during the stratification, with a concentration of methane up to 2,000 times higher in the bottom than in the surface during October. This vertical C_{CH_4} gradient, which has also been observed in other stratified freshwater ecosystems, is likely a result of (i) CH_4 production in anoxic sediments and its hypolimnetic accumulation, (ii) the existence of a strong and sharp thermal stratification, that prevents the whole lake water circulation, and (iii) methane oxidation that may have occurred with high intensity in the oxycline due to the absence of subtract limitation (Utsumi *et al.* 1998). Even though methane oxidation was not measured in this study, it was inferred by the existence of inversely proportional C_{CH_4} and DO profiles. Over time, a high accumulation of CH_4 was observed in the anoxic hypolimnion of VB during the stratification (as also reported elsewhere, e.g., Bartosiewicz *et al.* 2016; Gerardo-Nieto *et al.* 2017; Thalasso *et al.* 2020), which outlines the importance of limnological dynamics on the concentration distribution of GHG in freshwater water bodies.

The surface C_{CH_4} varied only from 0.015 to 0.2795 µmol L^{-1} during the stratification period, values similar to the lower C_{CH_4} reported for other tropical ecosystems (Engle & Melack 2000), particularly those with a similar size range (5–50 km^2), and that are deep enough to allow water column stratification (Kankaala *et al.* 2013).

Nevertheless, in all the sampled seasons, C_{CH_4} was higher than the equilibrium value with the current atmospheric CH_4 concentration of 1.82 ppmv (average concentration measured 1 m above the surface), indicating a permanent oversaturation of CH_4. These oversaturation surface concentrations provide a clear indication that VB behaved as a source of CH_4 even

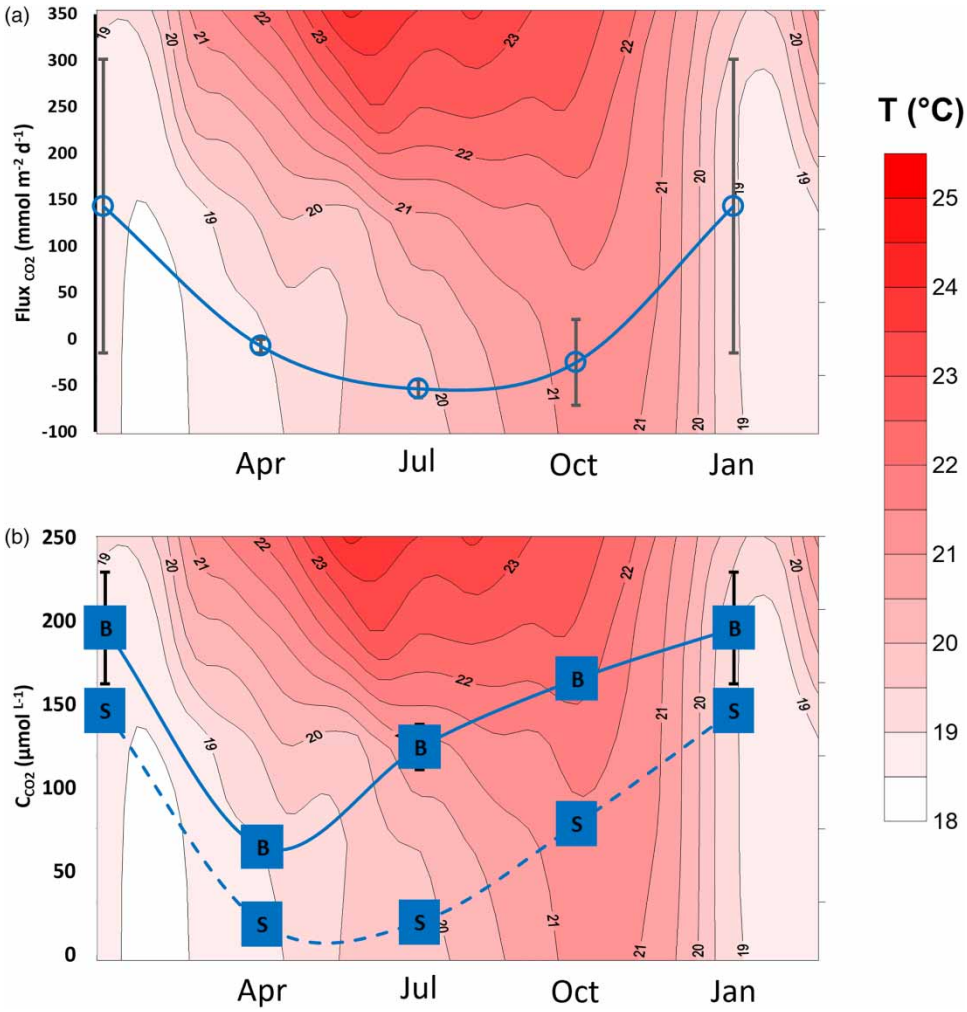

Figure 5 | CO_2 seasonal dynamics in Valle de Bravo: (a) seasonal variation of mean CO_2 fluxes, and (b) seasonal mean C_{CO_2}. Dashed line and S symbols indicate surface C_{CO_2}, solid line and B symbols indicate bottom C_{CO_2}, and vertical lines depict the standard deviation. The plots are drawn over the temperature vertical distribution to help outline the effect of the limnological dynamics of the lake reservoir on the gas concentration and fluxes.

during the stratification, which was also confirmed by the CH_4 flux measurements, which are discussed further ahead. In spite of the occurrence of CH_4 emission during the stratification, CH_4 accumulated in the hypolimnion of the lake, and the bottom C_{CH_4} reached levels much higher than at the surface, ranging from 0.292 to 176.808 µmol L^{-1} (with a higher inter-sample variation; CV = 115%), outlining an important hypolimnetic CH_4 storage in VB during the stratification period.

In fact, the increase of the bottom C_{CH_4} during stratification reached up to 153.097 µmol L^{-1} in the October sampling, which was prior to the overturn of the reservoir. Assuming that the C_{CH_4} measured in the bottom was similar for the entire hypolimnion, based on the high stability and homogeneity previously reported for VB (Merino-Ibarra *et al.* 2008), a total CH_4 mass accumulation of 250.57 Ton for the entire system was estimated. Considering the surface area of VB during the October sampling, the storage contribution was 0.971 mol CH_4 m^{-2}. This storage mass would then have been released during the overturn that took place between the October 2019 and January 2020 samplings, as previously reported for other ecosystems (Bartosiewicz *et al.* 2015).

A positive correlation between temperature (near the sediments) and C_{CH_4} was found (R^2 of 0.92), which is consistent with the temperature dependence of the methanogenic community. Methanogenesis is a mesophilic process, in which higher temperatures imply higher CH_4 production rates, with an optimum temperature between 35 and 40 °C (Schulz *et al.* 1997; Yvon-Durocher *et al.* 2014). This allows identifying a connection between water level decrease and CH_4 emissions in VB.

Since Merino-Ibarra *et al.* (2021) have shown that the rate of hypolimnetic warming in VB during stratification increases rapidly as the water level of the reservoir drops, the decrease of the water level – a scenario likely to become frequent due to climate change (Valdespino-Castillo *et al.* 2019) – would derive in an enhancement of CH_4 emissions in VB and water bodies that behave similarly.

The C_{CO_2} measured in the reservoir varied from 15.062 μmol L^{-1} (in the surface on April 2019) to 219.505 μmol L^{-1} (in the bottom, January 2020; Figure 5), with an annual average surface C_{CO_2} of 65.783 ± 60.525 μmol L^{-1}. As in the cases of C_{CH_4} and DO, when the reservoir was stratified, the C_{CO_2} in the bottom was significantly higher than in the surface ($p < 0.05$), and in the bottom of VB C_{CO_2} averaged overall 139.893 ± 57.207 μmol L^{-1}.

During the stratification, surface C_{CO_2} varied from 15.062 to 78.218 μmol L^{-1}, which are values within the order of magnitude reported previously for other tropical freshwater ecosystems (Marotta *et al.* 2010) and ecosystems with a similar size range (López Bellido *et al.* 2009; Kankaala *et al.* 2013). In contrast to the case of C_{CH_4}, during stratification, C_{CO_2} was below the value needed for equilibrium with the current atmospheric CO_2 concentration of 412 ppm (measured 1 m above the water surface). This surface sub-saturation of CO_2 provides an indication that VB behaved as a CO_2 sink during the stratification period, which was also confirmed by the negative CO_2 fluxes measured during that period, as will be discussed further ahead.

Bottom C_{CO_2} varied from 59.772 to 219.505 μmol L^{-1} in VB during 2019–2020, values also within the range of values reported for ecosystems with similar size range (Kankaala *et al.* 2013). However, bottom concentrations were always higher than at the surface, and C_{CO_2} exhibited a similar trend than C_{CH_4} and DO, due to CO_2 accumulation in the anoxic hypolimnion. The hypolimnetic C_{CO_2} reached up to 165.188 ± 4.977 μmol L^{-1} during October. Assuming C_{CO_2} bottom concentration was similar throughout the hypolimnion, based on the high stability and homogeneity reported by Merino-Ibarra *et al.* (2008), a total CO_2 mass accumulation of 390.11 ton for the whole lake was estimated, which is equivalent to 0.537 mol CO_2 m^{-2} considering its surface area in October 2019.

CH_4 and CO_2 fluxes

No evidence of ebullition was detected in VB during any of the sampling campaigns, either by visual observation or during SC measurement. This could be in part due to the fact that our monitoring station was near the center of the reservoir and at a depth greater than 20 m, where ebullition fluxes are less commonly observed (Natchimuthu *et al.* 2016; West *et al.* 2016). However, the existence of ebullitive GHG emissions cannot be totally discarded in VB, mainly in the case of CH_4 due to its low solubility in water (mole fraction solubility of 2.81×10^{-5} at 20 °C), and because ebullition events occur on a time frame of seconds and are followed by long periods without ebullition events (Saunois *et al.* 2016; Gerardo-Nieto *et al.* 2019). So, our estimates on CH_4 emissions are a minimum, a lower bound, and could be higher if there were any ebullition events that went undetected.

CH_4 emissions from VB varied between 23.25 μmol m^{-2} day^{-1} in the October sampling (before the onset of the diurnal wind) and 1,220.80 μmol m^{-2} day^{-1} in April, after the onset of the diurnal wind. As we mentioned in the methods section, GHG fluxes were measured before and after the onset of the strong diurnal wind. Figure 4 shows that the methane emissions from VB are higher after the onset of the diurnal wind in all seasons. These higher CH_4 fluxes are likely a result of the wind speed effect on the surface gas exchange, since the water was oversaturated with CH_4 throughout the samplings in 2019–2020. These fluxes could also be enhanced by the boundary mixing events the daily wind drives in VB (Merino-Ibarra *et al.* 2021), and less likely by any bottom currents – which are prone to CH_4 liberation (Joyce & Jewell 2003) – that may derive from internal waves breaking against the bottom of VB, a mechanism that still would need to be assessed there.

The mean seasonal CH_4 flux measured was 816.64 ± 571.56 μmol m^{-2} day^{-1} in April, 125.11 ± 40.08 μmol m^{-2} day^{-1} in July, 140.14 ± 165.31 μmol m^{-2} day^{-1} in October, and 444.36 ± 562.08 in January. Assuming that each of the four campaigns was equally representative of one quarter of the year, the annual CH_4 emissions from VB derived from direct measurements would be 0.139 mol m^{-2} $year^{-1}$, which implies 36.76 ton CH_4 for the entire reservoir. This is to be added to the storage component of the annual flux, which is the main way CH_4 is released from reservoirs (Kemenes *et al.* 2007). As previously calculated, VB would release on an annual basis a total of 287.33 ton CH_4 to the atmosphere, 87.21% of which is released during the autumn overturn.

Figure 5 shows the CO_2 fluxes, which varied between −60.11 mmol m^{-2} day^{-1} (July, before the onset of the diurnal wind) and 254.99 mmol m^{-2} day^{-1} (January, after the onset of the diurnal wind). As in the case of CH_4 fluxes, in all the sampling campaigns, the CO_2 fluxes were higher after the onset of the diurnal wind, supporting the importance of physical processes and the limnological dynamics for the emission rates, particularly the epilimnetic wind mixing, and the boundary mixing

events driven by the shoaling of the pycnocline with the bottom and shoreline (Merino-Ibarra *et al.* 2021). Considering the measurements before and after the wind onset, the means of seasonal CO_2 fluxes were -7.39 ± 7.53 mmol m^{-2} day^{-1} in April, $-53.36.11 \pm 9.54$ mmol m^{-2} day^{-1} in July, -25.05 ± 46.07 mmol m^{-2} day^{-1} in October, and 143.26 ± 158.01 mmol m^{-2} day^{-1} in January.

The negative CO_2 fluxes observed in VB throughout the stratification are consistent with the high autotrophic condition of the epilimnion of the reservoir during this limnological period (Valdespino-Castillo *et al.* 2014; Guimarais-Bermejo *et al.* 2018), which drives a CO_2 assimilation rate high enough to maintain continuously subsaturated C_{CO_2} values at the surface, in spite of the enhancement of the atmospheric CO_2 flux that the alkalinity of VB would cause (Wanninkhof & Knox 1996). In spite of the high productivity of the epilimnion during the stratification period, when the reservoir operates as a CO_2 sink, the net annual heterotrophy of the reservoir lake (Valdespino-Castillo *et al.* 2014; Guimarais-Bermejo *et al.* 2018) implies that overall it will behave as a net source of CO_2, with a very strong pulse of CO_2 emission during the turnover period and the lake circulation, as the high flux (143.26 ± 158.01 mmol m^{-2} day^{-1}) observed in January supports.

Assuming that each of the four campaigns was equally representative of one quarter of the year, the calculated average annual CO_2 emission from VB was 5.24 mol m^{-2} $year^{-1}$, which implies an annual emission of 3,806.22 Ton CO_2 for the entire reservoir lake per year. Additionally, the storage component must also be included, and once it is calculated as previously described and added, a total emission of 4,196.34 Ton of CO_2 from VB on a yearly basis was calculated, of which in this case only 9.30% of it would be released during the circulation period. This proportion contrasts with the case of CH_4, where most (~87%) of the emission occurs during the overturn.

To integrate the GHG emissions of CH_4 and CO_2 from VB here calculated, and to assess their relative contribution to global warming, both emissions were converted to CO_2 equivalents. Table 2 summarizes the emissions from VB. Overall, the GHG total emissions from VB expressed in CO_2 equivalents (CO_{2eq}; 25 g CO_{2eq} g^{-1} CH_4; Shindell *et al.* 2009) were calculated at 11,379.619 ton CO_{2eq} on an annual basis, 63.12% of which corresponds to CH_4 (Table 2). This proportion is similar to that suggested by Tranvik *et al.* (2009), who considered equal CH_4 and CO_2 contributions. However, these results contrast with those reported by Holgerson & Raymond (2016) who found that the contribution of CH_4 (in CO_2 eq) in diffusive fluxes depends on the lake area, and in the case of lakes with areas from 10 to 100 km^2, as is the case of VB, the CH_4 contributes less than 5% of total emission. In this sense, VB has a much higher relative contribution of CH_4 that is an order of magnitude higher.

Another consequence of the high relative contribution of CH_4 is that the that the overturn release of the hypolimnetic (deep) GHG accumulated during the stratification period represents 58.48% of the total GHG emissions of VB (Table 2).

These results show that hypertrophic reservoirs like VB can be emitting a much higher relative amount of CH_4 than would be expected for their relatively small surface area (Holgerson & Raymond 2016). They also reveal that a strong wing regime as found in VB can enhance the emissions as the fluxes measured before and after the onset of the wind in VB clearly show. Systems with a strong wind regime would be emitting faster, while systems with light winds may have higher storage that would be released during extreme weather events.

This case study also shows that water level changes, which are likely to increase in the near future due to the effects of climate change can also enhance the GHG emissions from the bottom of the systems, either due to reduced pressure that would allow ebullition, to increased vertical mixing and to the enhancement of methanogenesis due to the bottom temperature increase derived from vertical mixing or to overall warming of reservoirs.

Table 2 | GHG (CH_4 and CO_2) emissions from VB reservoir lake expressed as g CO_{2eq} m^{-2} day^{-1}

	CH_4 (gCO_{2eq} m^{-2} day^{-1})				CO_2 (gCO_2 m^{-2} day^{-1})			
Emission pathway	**Apr**	**Jul**	**Oct**	**Jan**	**Apr**	**Jul**	**Oct**	**Jan**
Diffusive flux	0.326 ± 0.228	0.050 ± 0.016	0.056 ± 0.066	0.177 ± 0.224	-0.325 ± 0.331	-2.348 ± 0.420	-1.102 ± 2.027	6.303 ± 6.952
Storage Flux	1.042 ± 0.233				0.065 ± 0.003			
Total annual flux	1.193 ± 0.367				0.696 ± 0.006			
Total annual GHG emissions	1.889 ± 0.335							

These effects should be considered by water managers along with their water administration considerations, as the impact and the likely feedback on climate change they may have could be of greater importance that the water management priorities themselves.

CONCLUSIONS

The annual CH_4 and CO_2 dynamics monitored in VB during 2019–2020 are overall consistent with previously reported work on the carbon dynamics of tropical freshwater bodies of a similar size range, although in VB, the relative importance of CH_4 was much higher, accounting for half of the carbon emissions, one order of magnitude higher than previously expected. In spite of this and of the highly eutrophic condition of VB, the overall GHG emissions observed in 2019–2020 in this reservoir were close to the center of the range of values previously reported for lakes with a similar size. A GHG emission of 1.889 $gCO_{2eq}\ m^{-2}\ year^{-1}$ was calculated, corresponding to a total emission from VB of 11,379.619 ton CO_{2eq} on an annual basis, ~63% of which would correspond to CH_4 emissions.

In VB, the strong diurnal winds that characterize this reservoir lake enhanced the emission rates, pointing out an important effect of wind that should be accounted for in the scope of the climate changes to come. Seasonal monitoring in VB also revealed that the mixing regime and the limnological dynamics of water bodies have important effects on their greenhouse gas emissions. On the short scale, water levels that can alter both the intensity of boundary mixing events and the local warming rate are also important factors that can affect GHG emissions. In the VB reservoir lake, thermal stratification narrowed down the CH_4 emissions, and the CO_2 fluxes were negative. Therefore, VB functioned as a net sink of GHG during the stratification period. As a result, GHG accumulated in the hypolimnion until the winter overturn of the lake, and the emissions derived from the storage of GHG in the lake represented a large fraction (more than 58%) of total annual fluxes. Stratification storage and overturn emission were particularly important in the case of CH_4, for which most (~87%) of its emission was due to this storage and its emission during the overturn period, outlining the importance of limnological dynamics on CH_4 emission from stratifying water bodies. Because of the importance of wind and mixing events, future work should be directed to understand the short-scale emissions that may occur associated with these two critical factors.

ACKNOWLEDGEMENTS

We acknowledge CONAHCYT (project CF-2023-G-155, Postdoctoral scholarships to O. G-N, P.M V-C and J.A. R-Z), and UNAM (PAPITT IN111321 and PASPA, DGAPA, UNAM to M.M-I.) for their funding. We also acknowledge 'Patronato Pro-Valle de Bravo A.C.' and Club Naútico Avándaro A.C. for their logistical support, and many students and collaborators, including Jaqueline Hernández-Angeles, Ariadna Esther Gómez Montesinos, Adriana Hernández Cruz, Zubia Jocelyn Cisneros Ramos. and many others for their collaboration in the field and laboratory work needed for this publication

FUNDING

This work was funded by CONAHCYT through project CF-2023-G-155 and PAPITT IN111321 from DGAPA, UNAM. Authors also acknowledge individual funding received: O. G-N. and P.M.V-C. were supported by CONAHCYT (#747276), and M.M-I. by PASPA of DGAPA, UNAM. The funding from these sponsors made possible the writing, review, and publishment of this paper, but they did not have any involvement in the study design, in the collection, analysis and interpretation of data, in the writing of the report, and in the decision to submit the article for publication.

DATA AVAILABILITY STATEMENT

All relevant data are included in the paper or its Supplementary Information.

CONFLICT OF INTEREST

The authors declare there is no conflict.

REFERENCES

Barjau-Aguilar, M., Merino-Ibarra, M., Ramírez-Zierold, J. A., Castillo-Sandoval, S. F., Vilaclara-Fatjó, G., Guzmán-Arias, A. P., Macek, M., Alcántara-Hernández, R. J., Sánchez-Carrillo, S., Valdespino-Castillo, P. M., Sacristán-Ramírez, A., Quintanilla-Terminel, J. G., Monroy-Ríos, E., Díaz-Valenzuela, J., Lestayo-González, J. A., Gerardo-Nieto, O. A. & Zayas, R. G. D. 2022 Nitrogen and phosphorous retention

in tropical eutrophic reservoirs with water level fluctuations: A case study using mass balances on a long-term series. *Water (Switzerland)* **14** (14). https://doi.org/10.3390/w14142144.

Bartlett, K. B. & Harriss, R. C. 1993 Review and assessment of methane emissions from wetlands. *Chemosphere* **26**, 261–320. https://doi.org/10.1017/CBO9781107415324.004.

Bartosiewicz, M., Laurion, I. & MacIntyre, S. 2015 Greenhouse gas emission and storage in a small shallow lake. *Hydrobiologia* **757** (1), 101–115. https://doi.org/10.1007/s10750-015-2240-2.

Bartosiewicz, M. I., Laurion, I., Clayer, F. & Maranger, R. 2016 Heat-wave effects on oxygen, nutrients, and phytoplankton can alter global warming potential of gases emitted from a small shallow lake. *Environmental Science and Technology* **50** (12), 6267–6275. https://doi.org/10.1021/acs.est.5b06312.

Bastviken, D., Ejlertsson, J. & Tranvik, L. 2002 Measurement of methane oxidation in lakes: A comparison of methods. *Environmental Science & Technology* **36** (15), 3354–3361. Available from: http://www.ncbi.nlm.nih.gov/pubmed/12188365.

Branco, C. W. C., Kozlowsky-Suzuki, B., Sousa-Filho, I. F., Guarino, A. W. S. & Rocha, R. J. 2009 Impact of climate on the vertical water column structure of Lajes Reservoir (Brazil): A tropical reservoir case. *Lakes & Reservoirs: Research & Management* **14** (3), 175–191. https://doi.org/10.1111/j.1440-1770.2009.00403.x.

Coloso, J. J., Cole, J. J. & Pace, M. L. 2011 Short-term variation in thermal stratification complicates estimation of lake metabolism. *Aquatic Sciences* **73** (2), 305–315. https://doi.org/10.1007/s00027-010-0177-0.

Deemer, B. R., Harrison, J. A., Li, S., Beaulieu, J. J., Delsontro, T., Barros, N., Bezerra-Neto, J. F., Powers, S. M., Dos Santos, M. A. & Vonk, J. A. 2016 Greenhouse gas emissions from reservoir water surfaces: A new global synthesis. *BioScience* **66** (11), 949–964. https://doi.org/10.1093/biosci/biw117.

Encinas Fernández, J., Peeters, F. & & Hofmann, H. 2014 Importance of the autumn overturn and anoxic conditions in the hypolimnion for the annual methane emissions from a temperate lake. *Environmental Science and Technology* **48** (13), 7297–7304. https://doi.org/10.1021/es4056164.

Engle, D. & Melack, J. M. 2000 Methane emissions from an Amazon floodplain lake: Enhanced release during episodic mixing and during falling water. *Biogeochemistry* **51** (1), 71–90. https://doi.org/10.1023/A:1006389124823.

Fendinger, N. J., Adams, D. D. & Glotfelty, D. E. 1992 The role of gas ebullition in the transport of organic contaminants from sediments. *Science of the Total Environment* **112** (2–3), 189–201. https://doi.org/10.1016/0048-9697(92)90187-W.

Gerardo-Nieto, O., Astorga-España, M. S., Mansilla, A. & Thalasso, F. 2017 Initial report on methane and carbon dioxide emission dynamics from sub-Antarctic freshwater ecosystems: A seasonal study of a lake and a reservoir. *Science of the Total Environment* **593**, 144–154. https://doi.org/10.1016/j.scitotenv.2017.02.144.

Gerardo-Nieto, O., Vega-Peñaranda, A., Gonzalez-Valencia, R., Alfano-Ojeda, Y. & Thalasso, F. 2019 Continuous measurement of diffusive and ebullitive fluxes of methane in aquatic ecosystems by an open dynamic chamber method. *Environmental Science and Technology* **53** (9), 5159–5167. https://doi.org/10.1021/acs.est.9b00425.

Glissmann, K., Chin, K., Casper, P. & Conrad, R. 2004 Methanogenic pathway and archaeal community structure in the sediment of eutrophic lake Dagow : Effect of temperature. *Microbial Ecology* **48** (1), 389–399. https://doi.org/10.1007/s00248-003-2027-2.

Guimarais-Bermejo, M. O., Merino-Ibarra, M., Valdespino-Castillo, P. M., Castillo-Sandoval, F. S. & Ramírez-Zierold, J. A. 2018 Metabolism in a deep hypertrophic aquatic ecosystem with high water-level fluctuations: A decade of records confirms sustained net heterotrophy. *PeerJ* **6**, e5205. https://doi.org/10.7717/peerj.5205.

Holgerson, M. A. & Raymond, P. A. 2016 Large contribution to inland water CO_2 and CH_4 emissions from very small ponds. *Nature Geoscience* **9** (3), 222–226. https://doi.org/10.1038/ngeo2654.

Hrsak, D. & Begonja, A. 1998 Growth characteristics and metabolic activities of the methanotrophic-heterotrophic groundwater community. *Journal of Applied Microbiology* **85** (3), 448–456. https://doi.org/10.1046/j.1365-2672.1998.853505.x.

Joyce, J. & Jewell, P. W. 2003 Physical controls on methane ebullition from reservoirs and lakes. *Environmental and Engineering Geoscience* **9** (2), 167–178. https://doi.org/10.2113/9.2.167.

Kalff, J. 2002 *Limnology – Inland Water Ecosystems*, Vol. 21, Issue 2. Prentice-Hall, NJ. https://doi.org/10.2307/1468422.

Kankaala, P., Huotari, J., Tulonen, T. & Ojala, A. 2013 Lake-size dependent physical forcing drives carbon dioxide and methane effluxes from lakes in a boreal landscape. *Limnology and Oceanography* **58** (6), 1915–1930. https://doi.org/10.4319/lo.2013.58.6.1915.

Kemenes, A., Forsberg, B. R. & Melack, J. M. 2007 Methane release below a tropical hydroelectric dam. *Geophysical Research Letters* **34** (12), 1–5. https://doi.org/10.1029/2007GL029479.

Linstrom, P. J. & Mallard, W. 2016 *NIST Chemistry WebBook, NIST Standard Reference Database Number 69*, National Institute of Standards and Technology, Gaithersburg MD, 20899, https://doi.org/10.18434/T4D303, (accessed 22 December 2023).

Livingston, G. P. & Hutchinson, G. L. 1995 Enclosure-based measurement of trace gas exchange: Applications and sources of error. In: *Biogenic Trace Gases: Measuring Emissions From Soil and Water*. Blackwell Science, pp. 14–50.

López Bellido, J., Tulonen, T., Kankaala, P. & & Ojala, A. 2009 CO_2 and CH_4 fluxes during spring and autumn mixing periods in a Boreal lake (Pääjärvi, Southern Finland). *Journal of Geophysical Research: Biogeosciences* **114** (4), 1–12. https://doi.org/10.1029/2009JG000923.

Magen, C., Lapham, L. L., Pohlman, J. W., Marshall, K., Bosman, S., Casso, M. & Chanton, J. P. 2014 A simple headspace equilibration method for measuring dissolved methane. *Limnology and Oceanography: Methods* **12** (9), 637–650. https://doi.org/10.4319/lom.2014.12.637.

Marcé, R., Obrador, B., Morguí, J. A., Lluís Riera, J., López, P. & Armengol, J. 2015 Carbonate weathering as a driver of CO_2 supersaturation in lakes. *Nature Geoscience* **8** (2), 107–111. https://doi.org/10.1038/ngeo2341.

Marotta, H., Duarte, C. M., Meirelles-Pereira, F., Bento, L., Esteves, F. A. & Enrich-Prast, A. 2010 Long-term CO_2 variability in two shallow tropical lakes experiencing episodic eutrophication and acidification events. *Ecosystems* **13** (3), 382–392. https://doi.org/10.1007/s10021-010-9325-6.

Merino-Ibarra, M., Monroy-Ríos, E., Vilaclara, G., Castillo, F. S., Gallegos, M. E. & Ramírez-Zierold, J. 2008 Physical and chemical limnology of a wind-swept tropical highland reservoir. *Aquatic Ecology* **42** (3), 335–345. https://doi.org/10.1007/s10452-007-9111-5.

Merino-Ibarra, M., Ramírez-Zierold, J. A., Valdespino-Castillo, P. M., Castillo-Sandoval, F. S., Guzmán-Arias, A. P., Barjau-Aguilar, M., Monroy-Ríos, E., López-Gómez, L. M., Sacristán-Ramírez, A., Quintanilla-Terminel, J. G., Zayas, R. G. D., Jimenez-Contreras, J., Valeriano-Riveros, M. E., Vilaclara-Fatjó, G. & Sánchez-Carrillo, S. 2021 Vertical boundary mixing events during stratification govern heat and nutrient dynamics in a windy tropical reservoir lake with important water-level fluctuations: A long-term (2001–2021) study. *Water* **13**, 21. https://doi.org/10.3390/w13213011.

Miller, D. N., Yavitt, J. B., Madsen, E. L. & Ghiorse, W. C. 2004 Methanotrophic activity, abundance, and diversity in forested swamp pools: Spatiotemporal dynamics and influences on methane fluxes. *Geomicrobiology Journal* **21** (4), 257–271. https://doi.org/10.1080/01490450490438766.

Natchimuthu, S., Sundgren, I., Gålfalk, M., Klemedtsson, L., Crill, P., Danielsson, Å. & Bastviken, D. 2016 Spatio-temporal variability of lake CH_4 fluxes and its influence on annual whole lake emission estimates. *Limnology and Oceanography* **61** (S1), S13–S26. https://doi.org/10.1002/lno.10222.

Padisák, J., Barbosa, F., Koschel, R. & Krienitz, L. 2003 Deep layer cyanoprokaryota maxima in temperate and tropical lakes. *Advances in Limnology* **58**, 175–199. Available from: http://www.scopus.com/inward/record.url?eid=2-s2.0-1242265638&partnerID=tZOtx3y1

Podgrajsek, E., Sahlée, E. & Rutgersson, A. 2014 Diurnal cycle of lake methane flux. *Journal of Geophysical Research: Biogeosciences* **119** (3), 236–248. https://doi.org/10.1002/2013JG002327.

Ramírez-Zierold, J. A., Merino-Ibarra, M., Monroy-Ríos, E., Olson, M., Castillo, F. S., Gallegos, M. E. & Vilaclara, G. 2010 Changing water, phosphorus and nitrogen budgets for Valle de Bravo reservoir, water supply for Mexico City Metropolitan Area. *Lake and Reservoir Management* **26**, 23–34. https://doi.org/10.1080/07438140903539790.

Saunois, M., Bousquet, P., Poulter, B., Peregon, A., Ciais, P., Canadell, J. G., Dlugokencky, E. J., Etiope, G., Bastviken, D., Houweling, S., Janssens-Maenhout, G., Tubiello, F. N., Castaldi, S., Jackson, R. B., Alexe, M., Arora, V. K., Beerling, D. J., Bergamaschi, P., Blake, D. R., Brailsford, G., Brovkin, V., Bruhwiler, L., Crevoisier, C., Crill, P., Curry, C., Frankenberg, C., Gedney, N., Höglund-Isaksson, L., Ishizawa, M., Ito, A., Joos, F., Kim, H. S., Kleinen, T., Krummel, P., Lamarque, J. F., Langenfelds, R., Locatelli1, R., Machida, T., Maksyutov, S., McDonald, K. C., Marshall, J., Melton, J. R., Morino, I., O'Doherty, S., Parmentier, F. J. W., Patra, P. K., Peng, C., Peng1, S., Peters, G. P., Pison1, I., Prigent, C., Prinn, R., Ramonet1, M., Riley, W. J., Saito, M., Schroeder, R., Simpson, I. J., Spahni, R., Steele, P., Takizawa, A., Thornton, B. F., Tian, H., Tohjima, Y., Viovy1, N., Voulgarakis, A., van Weele, M., van der Werf, G., Weiss, R., Wiedinmyer, C., Wilton, D. J., Wiltshire, A., Worthy, D., Wunch, D. B., Xu, X., Yoshida, Y., Zhang, B., Zhang, Z. & Zhu, Q. 2016 The global methane budget: 2000–2017. *Earth System Science Data* **12** (3), 1561–1623.

Schulz, S., Matsuyama, H. & Ralf, C. 1997 Temperature dependence of methane production from different precursors in a profundal sediment (Lake Constance). *FEMS Microbiology Ecology* **22** (3), 207–213.

Shindell, D. T., Faluvegi, G., Koch, D. M., Schmidt, G. A., Unger, N. & Bauer, S. E. 2009 Improved attribution of climate forcing to emissions. *Science* **326** (5953), 716–718.

Thalasso, F., Sepulveda-Jauregui, A., Gandois, L., Martinez-Cruz, K., Gerardo-Nieto, O., Astorga-España, M. S., Teisserenc, R., Lavergne, C., Tananaev, N. & Barret, M. 2020 Sub-oxycline methane oxidation can fully uptake CH_4 produced in sediments: Case study of a lake in Siberia. *Scientific Reports* **10**, 1–7. https://doi.org/10.1038/s41598-020-60394-8.

Tranvik, L. J., Downing, J. A., Cotner, J. B., Loiselle, S. A., Striegl, R. G., Ballatore, T. J., Dillon, P., Finlay, K., Fortino, K. & Knoll, L. B. 2009 Lakes and reservoirs as regulators of carbon cycling and climate. *Limnology and Oceanography* **54** (6_part_2), 2298–2314. https://doi.org/10.4319/lo.2009.54.6_part_2.2298.

Utsumi, M., Nojiri, Y., Nakamura, T., Nozawa, T., Otsuki, A., Takamura, N., Watanabe, M. & Seki, H. 1998 Dynamics of dissolved methane and methane oxidation in Dimictic Lake Nojiri During Winter. *Limnology & Oceanography* **43** (1), 10–17. https://doi.org/10.4319/lo.1998.43.1.0010.

Valdespino-Castillo, P. M., Merino-Ibarra, M., Jiménez-Contreras, J., Castillo-Sandoval, F. S. & Ramírez-Zierold, J. A. 2014 Community metabolism in a deep (stratified) tropical reservoir during a period of high water-level fluctuations. *Environmental Monitoring and Assessment* **186** (10), 6505–6520. https://doi.org/10.1007/s10661-014-3870-y.

Valdespino-Castillo, P. M., Merino-Ibarra, M., Ramírez-Zierold, J. A., Castillo-Sandoval, F. S., González-De Zayas, R. & Carnero-Bravo, V. 2019 Towards the construction of a carbon fluxes inventory of tropical waters: A unifying method pipeline. Hacia el inventario de flujos de carbono en aguas tropicales: Unificar métodos. *Tecnología y Ciencias del Agua* **10** (1), 234–252. https://doi.org/10.24850/j-tyca-2019-01-09.

Valeriano-Riveros, M. E., Vilaclara, G., Castillo-Sandoval, F. S. & Merino-Ibarra, M. 2014 Phytoplankton composition changes during water level fluctuations in a high-altitude, tropical reservoir. *Inland Waters* **4** (3), 337–348. doi:10.5268/iw-4.3.598.

Verpoorter, C., Kutser, T., Seekell, D. A. & Tranvik, L. J. 2014 A global inventory of lakes based on high-resolution satellite imagery. *Geophysical Research Letters* **41** (18), 6396–6402. https://doi.org/10.1002/2014GL060641.

Vollenweider, R. A. & Kerekes, J. 1982 *Eutrophication of Waters: Monitoring. Assessment and Control*. OECD, Paris, p. 154.

Wanninkhof, R. & Knox, M. 1996 Chemical enhancement of CO_2 exchange in natural waters. *Limnology and Oceanography* **41** (4), 689–697.

West, W. E., Creamer, K. P. & Jones, S. E. 2016 Productivity and depth regulate lake contributions to atmospheric methane. *Limnology and Oceanography* **61** (S1), S51–S61. https://doi.org/10.1002/lno.10247.

Willmott, C. J. & Matsuura, K. 2006 On the use of dimensioned measures of error to evaluate the performance of spatial interpolators. *International Journal of Geographical Information Science* **20** (1), 89–102. https://doi.org/10.1080/13658810500286976.

Yvon-Durocher, G., Allen, A. P., Bastviken, D., Conrad, R., Gudasz, C., St-Pierre, A., Thanh-Duc, N. & del Giorgio, P. A. 2014 Methane fluxes show consistent temperature dependence across microbial to ecosystem scales. *Nature* **507** (7493), 488–491. https://doi.org/10.1038/nature13164.

First received 9 December 2023; accepted in revised form 8 February 2024. Available online 21 February 2024